

Geometrically Non-linear Analysis of Axisymmetric Plates and Shells

Cengiz POLAT and Zülfü Çınar ULUCAN

Firat University, Faculty of Engineering, Department of Civil Engineering,
23279, Elazig, TURKIYE
cpolat@firat.edu.tr

(Received: 27.02.2007; Accepted: 19.03.2007)

Abstract: A geometrically nonlinear formulation is presented for the axisymmetric plate and shell structures. The formulation is based on the total Lagrangian approach. The nonlinear equilibrium equations are solved using the Newton-Raphson method. Different numerical examples are performed to obtain the geometrically non-linear behaviour of axisymmetric plates and shells.

Keywords: Axisymmetric plate and shell, geometric nonlinearity, Newton-Raphson method.

Eksenel Simetrik Plak ve Kabukların Geometrik Bakımdan Lineer Olmayan Analizi

Özet: Plak ve kabuk yapılar için geometrik bakımdan lineer olmayan bir formülasyon verilmektedir. Formülasyonda toplam Lagrange yaklaşımı esas alınmaktadır. Lineer olmayan denge denklemleri Newton-Raphson metodu kullanılarak çözülmektedir. Eksenel simetrik plak ve kabukların geometrik bakımdan lineer olmayan davranışını elde etmek için değişik nümerik örnekler gerçekleştirilmiştir.

Anahtar kelimeler: Eksenel simetrik plak ve kabuk, geometrik bakımdan lineer olmayan davranış, Newton-Raphson metodu.

1. Introduction

In the linear analysis, the displacements and strains developed in the structure are small. That is, the geometry of the structure assumed remains unchanged during the loading process and linear strain approximations can be used. However, the geometry of the structure changes continuously during the loading process, and this fact is taken into account in the geometrically nonlinear analysis. In the linear analysis, the load carrying capacity of the structure cannot be predicted correctly. Therefore, it is necessary to use the non-linear equilibrium equations to describe the structural behaviour [1,2].

In this paper, the geometrically nonlinear behavior of axisymmetric plates and shells subjected to different axisymmetric loads for various shell parameters is studied. The total Lagrangian approach, in which all static and kinematic variables at the current state are referred to the initial configuration, is adopted. The nodal displacements are nonlinear functions of nodal rotations in the axisymmetric shell

formulation, thus restrictions of small nodal rotations during deformation process is removed. In the numerical application, the isoparametric axisymmetric shell elements are used. For such elements the element geometry is described in terms of the coordinates of middle surface nodes and the mid-surface nodal point normals. The incremental equations of equilibrium are solved by using the Newton-Raphson method. The nonlinear analysis of axisymmetric plates and shells is performed by a computer program which is written by the authors in MATLAB software.

2. Formulation

2.1. Kinematics of Deformation

For the isoparametric axisymmetric shell elements, mid-surface is defined by only two coordinates ξ and η . Figure 1 shows the nodal variables and the definitions of angles for a

typical node k in the element. The element geometry is defined by

$$x = \sum_{k=1}^n N_k x_k + \frac{\eta}{2} \sum_{k=1}^n N_k t_k \cos \varphi_k \quad (1)$$

$$y = \sum_{k=1}^n N_k y_k + \frac{\eta}{2} \sum_{k=1}^n N_k t_k \sin \varphi_k \quad (2)$$

where t_k is the element thickness at the node k , and n is the number of nodes in the element. For the finite element model, displacement field is approximated by using nodal displacements u_k and v_k , nodal rotation α_k , and the shape function N_k at the node k as follows;

$$u = \sum_{k=1}^n N_k u_k + \frac{\eta}{2} \sum_{k=1}^n N_k t_k F_{kx} \quad (3)$$

$$v = \sum_{k=1}^n N_k v_k + \frac{\eta}{2} \sum_{k=1}^n N_k t_k F_{ky} \quad (4)$$

and \mathbf{F}_k is defined by the following expression [3]

$$\mathbf{F}_k = \begin{Bmatrix} F_{kx} \\ F_{ky} \end{Bmatrix} = \begin{Bmatrix} \cos \varphi_k (\cos \alpha_k - 1) - \sin \varphi_k \sin \alpha_k \\ \sin \varphi_k (\cos \alpha_k - 1) + \cos \varphi_k \sin \alpha_k \end{Bmatrix} \quad (5)$$

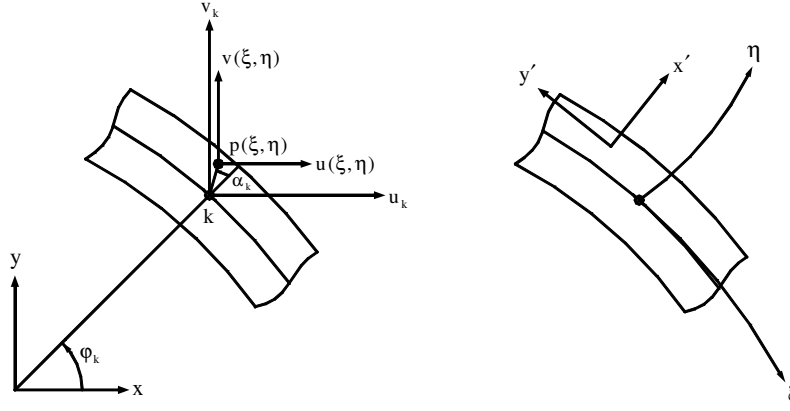


Figure 1. Definitions of angles and local axes of axisymmetric shell element

2.2. Nonlinear Finite Element Formulation

In the total Lagrangian approach, second Piola-Kirchhoff stresses and corresponding Green-Lagrange strains are considered [4]. It is assumed that shell thickness does not change during deformation that is, $\sigma_{x'}$ and $\varepsilon_{x'}$ can be neglected. For a linear elastic material, stresses and strains in the local coordinate system ($x'y'z$) can be written as

$$\boldsymbol{\sigma}' = \mathbf{D}' \boldsymbol{\varepsilon}' \quad (6)$$

$$\boldsymbol{\sigma}' = [\sigma_{x'} \quad \sigma_{y'} \quad \tau_{x'y'} \quad \sigma_{z'}]^T \quad (7)$$

$$\boldsymbol{\varepsilon}' = [\varepsilon_{x'} \quad \varepsilon_{y'} \quad \gamma_{x'y'} \quad \varepsilon_{z'}]^T \quad (8)$$

where \mathbf{D}' is the elasticity matrix in the local coordinate system and it can be obtained using these two assumptions $\sigma_{x'} = 0$ and $\varepsilon_{x'} = 0$. Similarly in the global coordinate system (xyz) stresses and strains are defined as

$$\boldsymbol{\sigma} = \mathbf{D} \boldsymbol{\varepsilon} \quad (9)$$

$$\boldsymbol{\sigma} = [\sigma_x \quad \sigma_y \quad \tau_{xy} \quad \sigma_z]^T \quad (10)$$

$$\boldsymbol{\varepsilon} = [\varepsilon_x \quad \varepsilon_y \quad \gamma_{xy} \quad \varepsilon_z]^T \quad (11)$$

where \mathbf{D} is the elasticity matrix in the global coordinate system and can be defined by

$$\mathbf{D} = \mathbf{T}\mathbf{D}'\mathbf{T}^T \quad (12)$$

where \mathbf{T} is the transformation matrix which is defined as

$$\mathbf{T} = \begin{bmatrix} c^2 & s^2 & -2sc & 0 \\ s^2 & c^2 & 2sc & 0 \\ sc & -sc & c^2 - s^2 & 0 \\ 0 & 0 & 0 & 1 \end{bmatrix} \quad (13)$$

where $c = \cos(a)$ and $s = \sin(a)$; a is the angle between the global x axis and the local x' axis in the undeformed configuration.

Green-Lagrange strains in the global coordinate system can be written as

$$\boldsymbol{\varepsilon} = \boldsymbol{\varepsilon}_0 + \boldsymbol{\varepsilon}_L \quad (14)$$

$$= \begin{bmatrix} u_x \\ v_y \\ u_y + v_x \\ \frac{u}{x} \end{bmatrix} + \begin{bmatrix} \frac{1}{2}[(u_x)^2 + (v_x)^2] \\ \frac{1}{2}[(u_y)^2 + (v_y)^2] \\ [u_x u_y + v_x v_y] \\ \frac{1}{2}\left[\left(\frac{u}{x}\right)^2\right] \end{bmatrix}$$

where $\boldsymbol{\varepsilon}_0$ and $\boldsymbol{\varepsilon}_L$ are the linear and nonlinear strains, respectively. If we define

$$\boldsymbol{\theta} = [u_x \quad v_x \quad u_y \quad v_y \quad u/x]^T \quad (15)$$

thus the linear and nonlinear strains of Eq. (14) can be written conveniently as

$$\boldsymbol{\varepsilon}_0 = \begin{bmatrix} 1 & 0 & 0 & 0 & 0 \\ 0 & 0 & 0 & 1 & 0 \\ 0 & 1 & 1 & 0 & 0 \\ 0 & 0 & 0 & 0 & 1 \end{bmatrix} \boldsymbol{\theta} = \mathbf{H}\boldsymbol{\theta} \quad (16)$$

$$\boldsymbol{\varepsilon}_L = \begin{bmatrix} u_x & v_x & 0 & 0 & 0 \\ 0 & 0 & u_y & v_y & 0 \\ u_y & v_y & u_x & v_x & 0 \\ 0 & 0 & 0 & 0 & u/x \end{bmatrix} \boldsymbol{\theta} = \frac{1}{2} \mathbf{A}\boldsymbol{\theta} \quad (17)$$

Taking the variation of the linear strain

$$d\boldsymbol{\varepsilon}_0 = \mathbf{H} d\boldsymbol{\theta} \quad (18)$$

and let

$$d\boldsymbol{\theta} = \mathbf{G} d\mathbf{u} \quad (19)$$

then, we can obtain the linear strain-displacement matrix \mathbf{B}_0 as

$$d\boldsymbol{\varepsilon}_0 = \mathbf{H}\mathbf{G} d\mathbf{u} = \mathbf{B}_0 d\mathbf{u} ; \quad \mathbf{B}_0 = \mathbf{H}\mathbf{G} \quad (20)$$

where the variation of the nodal parameters $d\mathbf{u}$ is given by

$$d\mathbf{u} = [du_1 \quad dv_1 \quad d\alpha_1 \quad \dots \quad du_k \quad dv_k \quad d\alpha_k]^T \quad (21)$$

$k = 1, 2, \dots, n$

Taking the variation of the nonlinear strain using Eq. (17)

$$d\boldsymbol{\varepsilon}_L = \frac{1}{2} d\mathbf{A}\boldsymbol{\theta} + \frac{1}{2} \mathbf{A} d\boldsymbol{\theta} \quad (22)$$

and we have

$$d\mathbf{A}\boldsymbol{\theta} = \mathbf{A} d\boldsymbol{\theta} \quad (23)$$

then

$$d\boldsymbol{\varepsilon}_L = \mathbf{A} d\boldsymbol{\theta} \quad (24)$$

If Eq. (24) is rewritten using Eq. (19), the nonlinear strain-displacement matrix \mathbf{B}_L can be obtained as

$$d\boldsymbol{\varepsilon}_L = \mathbf{A}\mathbf{G} d\mathbf{u} = \mathbf{B}_L d\mathbf{u} ; \quad \mathbf{B}_L = \mathbf{A}\mathbf{G} \quad (25)$$

Thus using Eq. (20) and Eq. (25), we can write

$$d\boldsymbol{\varepsilon} = \mathbf{B} d\mathbf{u} = (\mathbf{B}_0 + \mathbf{B}_L) d\mathbf{u} = [\mathbf{H} + \mathbf{A}] \mathbf{G} d\mathbf{u} \quad (26)$$

where \mathbf{B} is called as the strain-displacement matrix [5,6].

The equilibrium equation of the nonlinear system can be written as

$$\mathbf{R}(\mathbf{u}) = \int_V \mathbf{B}^T \boldsymbol{\sigma} dV - \mathbf{P} = \mathbf{F} - \Delta\lambda^{(i)} \mathbf{P} \quad (27)$$

where \mathbf{R} , \mathbf{F} and \mathbf{P} represent the out-of-balance force vector, the internal force vector and the externally applied load vector respectively, and $\Delta\lambda^{(i)}$ is the load-level parameter.

Taking the variation of Eq. (27) we have

$$d\mathbf{R} = \int_V d\mathbf{B}^T \boldsymbol{\sigma} dV + \int_V \mathbf{B}^T d\boldsymbol{\sigma} dV = \mathbf{K}_T d\mathbf{u} \quad (28)$$

and from Eq. (9) we can write

$$d\boldsymbol{\sigma} = \mathbf{D} d\boldsymbol{\varepsilon} = \mathbf{D} \mathbf{B} d\mathbf{u} \quad (29)$$

then Eq. (28) becomes

$$d\mathbf{R} = \int_V d\mathbf{B}^T \boldsymbol{\sigma} dV + \bar{\mathbf{K}} d\mathbf{u} \quad (30)$$

The matrix \mathbf{B} is defined by the Eq. (26), and the matrix $\bar{\mathbf{K}}$ is defined as

$$\bar{\mathbf{K}} = \int_V \mathbf{B}^T \mathbf{D} \mathbf{B} dV = \mathbf{K}_0 + \mathbf{K}_L \quad (31)$$

Substituting \mathbf{B}_0 and \mathbf{B}_L matrices into the first part in the right hand of the Eq. (30) instead of \mathbf{B} , that part can be written as

$$\begin{aligned} \int_V d\mathbf{B}^T \boldsymbol{\sigma} dV &= \int_V (d\mathbf{B}_0^T + d\mathbf{B}_L^T) \boldsymbol{\sigma} dV \\ &= \int_V (d\mathbf{G}^T \mathbf{H}^T + d\mathbf{G}^T \mathbf{A}^T + \mathbf{G}^T d\mathbf{A}^T) \boldsymbol{\sigma} dV \end{aligned} \quad (32)$$

or

$$\begin{aligned} \int_V d\mathbf{B}^T \boldsymbol{\sigma} dV &= (\mathbf{K}_{\sigma 2} + \mathbf{K}_{\sigma 3} + \mathbf{K}_{\sigma 1}) d\mathbf{u} \\ &= \mathbf{K}_{\sigma} d\mathbf{u} \end{aligned} \quad (33)$$

Hence, the Eq. (30) can be given as

$$\begin{aligned} d\mathbf{R} &= \mathbf{K}_{\sigma} d\mathbf{u} + \bar{\mathbf{K}} d\mathbf{u} \\ &= (\mathbf{K}_{\sigma} + \bar{\mathbf{K}}) d\mathbf{u} = \mathbf{K}_T d\mathbf{u} \end{aligned} \quad (34)$$

where \mathbf{K}_T is the tangent stiffness matrix and the explicit definition of this matrix can be found in the thesis of Polat [7].

2.3. Solution Method

In order to compute the nodal displacements, it is necessary to solve the system of nonlinear equilibrium equations using an incremental/iterative method. The load controlled Newton–Raphson method is the earliest method that is used to trace the equilibrium path [8]. This method is based on the linearization of the equilibrium equations at a prescribed load level, that is, $\Delta\lambda^{(i)}$ in Eq.(27) is kept constant during iterations. The iterations are performed until the residual is smaller than a prescribed tolerance. This method can trace the load–displacement curve before the occurrence of a limit point, but generally it will fail to converge beyond this point.

We adopted two convergence criterions together in the algorithm. One of them is the displacement-based convergence criterion and it can be written as

$$\|\Delta\mathbf{u}\| < \beta_u \|\mathbf{u}\| \quad (35)$$

where $\Delta\mathbf{u}$ are the iterative displacement changes, \mathbf{u} the total displacements and β_u prescribed tolerance. The norm of the iterative displacement change can be very small while the out-of-balance force norm is very large. To use only this criterion may result in some errors. Therefore, we used an additional convergence criterion known as energy-based convergence criterion of the form [9]

$$|\Delta\mathbf{u}^T \mathbf{R}| < \beta_r |\mathbf{u}^T (\Delta\lambda^{(i)} \mathbf{P})| \quad (36)$$

2.4. Numerical Examples

2.4.1. Geometric non-linear analysis of a clamped circular plate subjected to a uniformly distributed load: The large deformation analysis of a clamped circular plate subjected to a uniformly distributed load q with Poisson's ratio $\nu = 0.3$, Young's modulus $E = 1 \times 10^7$ MPa, radius $R = 100$ mm, and thickness $t = 2$ mm, is considered in this example. Linear (L2), quadratic (L3) and cubic

(L4) elements are used to model the circular plate (Fig 2.). The element matrices and the load vectors are formed using Gauss quadrature. 2×2 , 3×2 and 4×2 integration rules are employed for the linear, quadratic and cubic elements, respectively. Table I shows the center deflection of the plate for different elements and the analytical solution. In addition, in the Figure 3, the L3 element and the analytical solution results are compared. The results of the higher order elements are very close to the analytical solution.

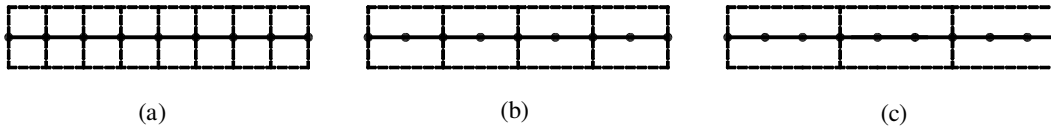


Figure 2. Meshes of a circular plate under uniform loading; a) eight linear element, b) four quadratic element, c) three cubic element.

Table I. Non-dimensional central deflection (v/t) of the circular plate with clamped boundaries under uniform load.

qR^4 / Et^4	L2	L3	L4	Analytical [10]
1	0.1500	0.1675	0.1675	0.1690
2	0.2906	0.3206	0.3206	0.3230
3	0.4176	0.4549	0.4550	0.4570
6	0.7210	0.7632	0.7632	0.7610
10	1.0055	1.0438	1.0438	1.0350
15	1.2615	1.2937	1.2937	1.2790

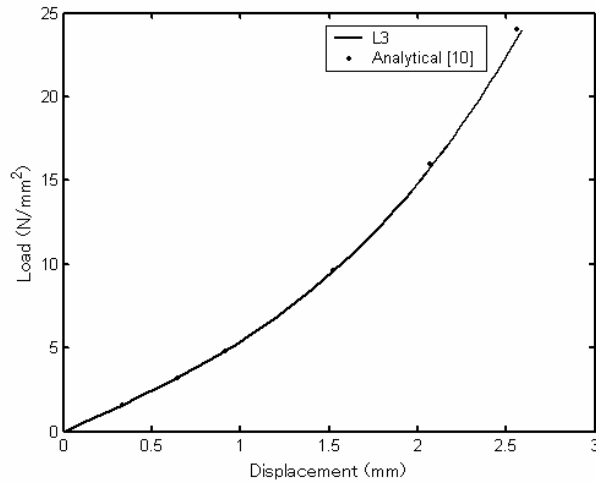


Figure 3. Central deflection of the circular plate.

2.4.2. Geometric non-linear analysis of a clamped circular plate subjected to a concentrated load at the centre of the plate:

The circular plate with the same geometric, material property and the same meshes as the one in Section 2.4.1 is subjected to a concentrated load at the centre. The non-dimensional central deflection of the circular

plate from the present elements by total Lagrangian formulation is compared with the analytical solution by Ref. [10] in Table II. The non-linear relationships between load and deflection are also shown in Figure 4. Also, the solution of the higher order elements is very close to the analytical solution for this problem.

Table II. Non-dimensional central deflection (v/t) of the circular plate with clamped boundaries under concentrated load.

Yük ($10^4 \times N$)	L2	L3	L4	Analytical [10]
1.6	0.1955	0.2129	0.2129	0.2129
3.2	0.3749	0.4035	0.4036	0.4049
4.8	0.5331	0.5674	0.5675	0.5695
6.4	0.6717	0.7084	0.7086	0.7098
8.0	0.7939	0.8314	0.8316	0.8309
9.6	0.9030	0.9405	0.9406	0.9372

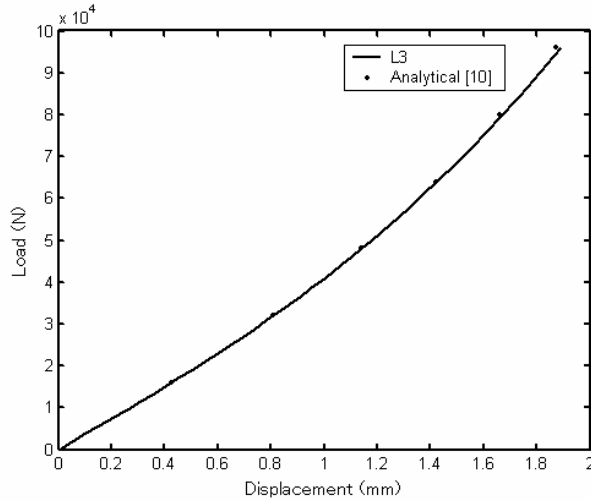


Figure 4. Central deflection of the circular plate

2.4.3. Geometric non-linear analysis of a clamped spherical cap under uniform external pressure: In Figure 5, the material and geometric properties of the spherical cap under uniform external pressure p are given. In the figure, λ is the shell parameter and p_0 the classical buckling pressure. Cubic shell elements are used to model the clamped spherical cap. The

element matrices and the load vectors are formed using Gauss quadrature with 4×2 integration rule. For different values of λ , dimensionless axisymmetric snap-through pressures p/p_0 of clamped spherical cap was investigated. Results were shown in Figure 6 with a reference solution. The obtained results are very close to the analytical solution.

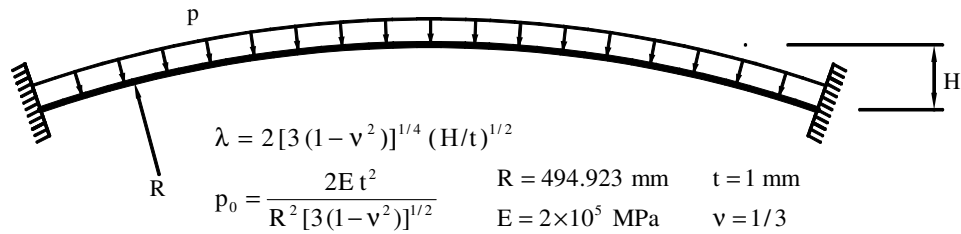


Figure 5. Geometric and material properties of the axisymmetric shell under uniform pressure.

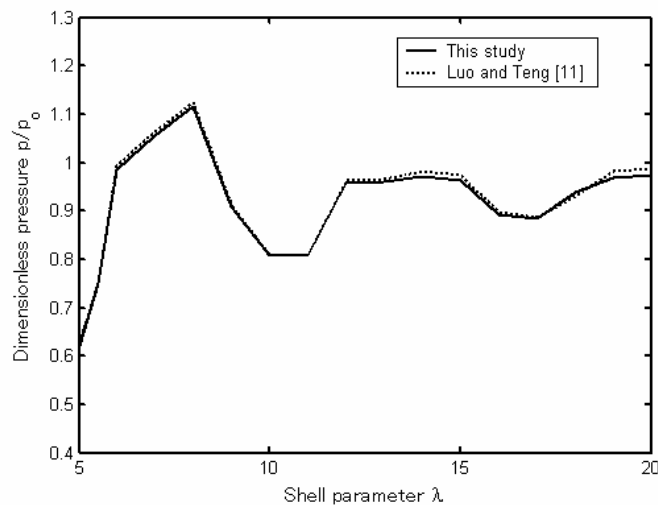


Figure 6. Comparison of present values of p/p_0 with those of Luo and Teng [11].

3. Conclusion

A geometrically nonlinear formulation based on total Lagrangian approach is given for the axisymmetric shell elements. Geometrically nonlinear behaviour of axisymmetric plates subjected to different loads are investigated. In

addition, axisymmetric snap-through pressures of clamped spherical caps also are studied under uniform pressure. The obtained results are similar to the analytical solution. Especially, those of the higher order elements give more accurate results.

References

- Zienkiewicz, O. C. (1977). The Finite-Element Method. 3rd edition, McGraw-Hill, London.
- Parente, E., Vaz., L. E. (2003). On Evaluation of Shape Sensitivities of Non-Linear Critical Loads. International Journal for Numerical Methods in Engineering, **56**(6), 809-846.
- Surana, K. S. (1982). Geometrically Nonlinear Formulation for the Axisymmetric Shell Elements. International Journal for Numerical Methods in Engineering, **18**, 477-502.
- Reddy, J. N. (1997). Mechanics of Laminated Composite Plates and Shells: Theory and Analysis. 2nd edition, CRC Press, New York.
- Polat, C., Calayır, Y. (2003). Sabit Dış Basınca Maruz Eksenel Simetrik Kabukların Geometrik

- Olarak Lineer Olmayan Analizi. XIII. Ulusal Mekanik Kongresi, 657-665, Gaziantep.
- 6 Polat, C., Calayir, Y., Ulucan, Z. Ç. (2006). Post-buckling Behavior of Geometrically Non-linear Axisymmetric Shells, Seventh International Congress on Advances in Civil Engineering, October 11-13, Yildiz Technical University, Istanbul, Turkey
- 7 Polat, C. (2006). Geometrik Bakımdan Lineer Olmayan Kabuk Yapıların Statik Ve Dinamik Davranışı, Doktora Tezi.
- 8 Memon, B. A., X. Z. Su. (2004). Arc-Length Technique for Nonlinear Finite Element Analysis. Journal of Zhejiang University, **5(5)**, 618-628.
- 9 Warren, J.E. (1997). Nonlinear Stability Analysis of Frame-Type Structures with Random Geometric Imperfections Using a Total-Lagrangian Finite Element Formulation, Ph. D. Thesis, Faculty of the Virginia Polytechnic Institute and State University, Virginia, 211p.
- 10 Zhang, Y. X., Cheung, Y. K. (2003). A Refined Non-Linear Non-Conforming Triangular Plate/Shell Element, International Journal for Numerical Methods in Engineering, **56**, 2387-2408.
- 11 Luo, Y. F., Teng, J.G. (1998). Stability Analysis of Shells of Revolution on Nonlinear Elastic Foundations. Computers and Structures, **69**, 499-511.